# Multizone Airflow Model in Modelica

Michael Wetter
United Technologies Research Center
411 Silver Lane
East Hartford, CT 06108

## Abstract

We present the implementation of a library of multizone airflow models in Modelica and a comparative model validation with CONTAM. Our models have a similar level of detail as the models in CONTAM and COMIS. The multizone airflow models allow modeling the flow between rooms through doors, staircases or construction cracks. The flow can be caused by buoyancy effects, such as stack effects in high rise buildings or air temperature imbalance between adjoining rooms, by flow imbalance of a ventilation system, or by wind pressure on the building envelope.

The here presented library can be used with a Modelica library for thermal building and HVAC system simulation to compute interzonal air flow rates. The combined use facilitates the integrated design of building systems, which is typically required for analyzing the interaction of room control loops in variable air volume flow systems through open doors, the flow in naturally ventilated buildings and the pressure in elevator shafts caused by stack effects.

*Keywords: Multizone Airflow, Contaminant Transport, Stack Effect*

## 1 Introduction

We present the implementation of a library of multizone airflow models in Modelica and a comparative model validation in which we computed the buoyancy driven air flow rates in CONTAM and in Modelica for a two storey building. The implemented models have a similar level of detail as the models in the state-of-the-art multizone airflow programs CONTAM [4] and COMIS [6]. Multizone airflow models consist of nodes that are connected by flow elements. The nodes may represent room air volumes, the exterior environment or connections in a duct system and contain state variables, typically pressure, temperature and concentrations such as water vapor, $CO_2$, smoke or pollutants.

The flow elements are airflow paths such as open doors and windows, construction cracks, stair cases, elevator shafts, ducts and fans.

Multizone airflow models are typically used for time domain simulation of convective energy and contaminant transport between thermal zones of a building and to quantify stack effects in high rise buildings. For thermal building simulation, the closed door and user-estimated airflows that are common practice in most multizone simulations are a poor representation of reality [8, 18]. Assessing the convective energy and species transport can also be important for controls analysis, since the convective transport through open doors can couple one local control loop with another. This situation may occur, for example, if two rooms have their own local VAV damper control loop that causes pressure or temperature imbalance if one damper closes. To model such phenomenas, the here presented airflow models can be used to define flow paths that connect different thermal zones of a building that may be presented by the model described in [23]. Multizone airflow models represent the room volumes assuming uniform distribution of temperature, pressure and species concentration throughout the room as opposed to the spatially more refined resolution of zonal models [10] or computational fluid dynamics models. The reduced number of state variables of multizone airflow models makes it computationally feasible to perform annual simulations of heat and species transport in buildings.

In [7], Feustel and Dieris present an extensive literature review and questionnary survey of more than 50 multizone airflow models and list the main equations used in those models. Today, two multizone airflow models are well established: CONTAM, developed by the National Institute of Standards and Technology (NIST) and COMIS, developed in 1988-89 in an international context within IEA Annex 23 at the Lawrence Berkeley National Laboratory (LBNL). COMIS has been interfaced with the thermal build-

ing energy simulation program EnergyPlus [9]. EnergyPlus uses airflow rates that were computed by COMIS in the previous time step. This coupling with time lagging, however, can cause instability if the time step is too large [18]. COMIS and CONTAM have both been implemented in TRNSYS in the form of a TRNSYS TYPE (i.e., a component model) that can be interfaced with TRNSYS' multizone thermal building model TYPE 56 [15]. In subsequent work, COMIS has also been integrated directly into TYPE 56 due to convergence problems and to improve the user interface [22]. The thermal building simulation programs IDA [19] and ESP-r [3, 8] have models for interzonal air exchange for bi-directional flow through open doors. The basic flow resistances used in COMIS, CONTAM, IDA and ESP-r are powerlaw equations that compute the steady-state flow as a function of the static pressure difference.

Lorenzetti [12] reports that some flow models in COMIS and CONTAM can give non-repeatable results due to memory in the calculation routines. For example, the crack model in COMIS finds the density of the air in the crack using the flow calculated in the last evaluation of the crack in question. This can cause the solver to fail converging to a solution. Another concern is that COMIS does not solve the mechanical energy balance and the friction models simultaneously which can yield to errors of around 30% for flows through passive vertical shafts for stairways, elevators or natural ventilation. Lorenzetti concludes that due to the decoupling of the mechanical energy balance and the friction models, COMIS cannot implement any meaningful model for bi-directional flow between floors of a building.

## 2 Physical Model Description

We use a powerlaw relationship to model the volume flow rate through an aperture as a function of the static pressure difference $\Delta P$ between two rooms. Let $\Delta P_{0,\varepsilon} \ll 1$ be a user specified parameter. The governing equations are

$$\dot{V} = \begin{cases} k\Delta P^m, & \text{for } \Delta P \geq 3/2\,\Delta P_{0,\varepsilon}, \\ -k(-\Delta P)^m, & \text{for } \Delta P \leq -3/2\,\Delta P_{0,\varepsilon}, \end{cases} \quad (1a)$$

where $\dot{V}$ is the volume flow rate, $k$ is a flow characteristics, $\Delta P$ is the static pressure difference over the aperture and $m \in [0.5,\ 1]$ is a flow exponent, with $m = 0.5$ for turbulent flow and $m = 1$ for laminar flow. For $m < 1$, the derivative $d\dot{V}/d\Delta P$ tends to infinity,

as $\Delta P \to 0$, which can cause problems for numerical solvers. Thus, we use for small pressure differences the linear function

$$\dot{V} = k\Delta P_{0,\varepsilon}^{m-1}\Delta P, \quad \Delta P \in [-\Delta P_{0,\varepsilon}/2,\ \Delta P_{0,\varepsilon}/2]. \quad (1b)$$

The transition between equation (1a) and (1b) is done in the intervals $\Delta P \in (-3/2\,\Delta P_{0,\varepsilon},\ -1/2\,\Delta P_{0,\varepsilon})$ and $\Delta P \in (1/2\,\Delta P_{0,\varepsilon},\ 3/2\,\Delta P_{0,\varepsilon})$ using the built-in Dymola function `spliceFunction`, which defines $\dot{V}(\cdot)$ as a function that is once continuously differentiable in $\Delta P$. Linearization around zero is also used in [4, 2].

We observed good numerical experiments by setting $\Delta P_{0,\varepsilon} = 0.1\,\text{Pa}$. Using $\Delta P_{0,\varepsilon} = 0.001\,\text{Pa}$ caused the time integration solver in some examples to jam at state events caused by a buoyancy driven flow reversal.

We will now discuss the implemented models, which all compute the flow based on (1).

### 2.1 Orifice

The flow through an orifice with cross section area $A$ can be deduced from the Bernoulli equation and is given by

$$\dot{V} = C_d A \sqrt{2/\rho}\,\Delta P^m, \quad (2)$$

where $C_d \in (0, 1)$ is a dimensionless discharge coefficient and $\rho$ is the density of the medium that flows through the orifice. Large openings are characterized by $m$ very close to 0.5, while values near 0.65 have been found for small crack-like openings [21, 4].

In [20], van der Mass et al. present a brief literature review about discharge coefficients and conducted own experiments on a 1:10 and a full scale model. They concluded that $C_d$ can confidently be chosen in the range of 0.6 to 0.75, provided that the temperature stratification in the rooms is taken into account (and hence $\dot{V}$ is obtained using the integration $\dot{V} = \int(d\dot{V}/dh)\,dh$ over the aperture height.) They report that $C_d = 0.61$ is widely used, and that Mahajan [14, 13] found values as low as 0.33 for isothermal rooms.[1] Van der Mass et al. also report that Riffat [17] found for the transport through both a door and a staircase a value of $C_d = 0.6$ for an interzonal air temperature difference of $\Delta T = 1\,\text{K}$, decreasing to $C_d = 0.25$ for $\Delta T = 10\,\text{K}$, which is in contrast to Kiel and Wilson [11], which obtained in full scale experiments $C_d = 0.40 + 0.0045\,\Delta T$.

---

[1] Two rooms are said to be isothermal if the temperature difference between the rooms is much larger than the vertical temperature difference between floor and ceiling in each room.
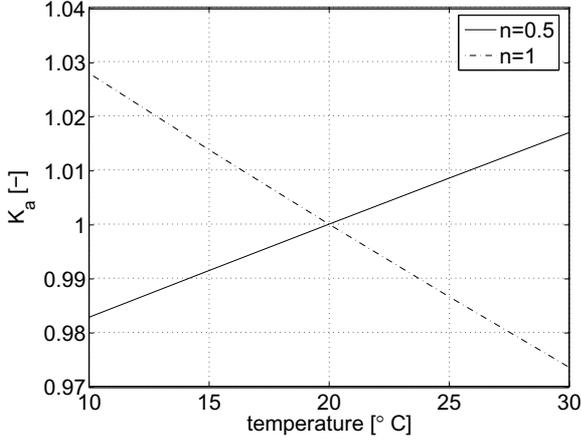
Figure 1: Correction factor used in CONTAM for change of volume flow rate as a function of temperature.

To account for the temperature dependency of the air density $\rho$ and the kinematic viscosity $\nu$, CONTAM multiplies the right hand side of the orifice equation (2) by the correction factor

$$K_a(P,T) = \left(\frac{\rho_0}{\rho(P,T)}\right)^n \left(\frac{\nu_0}{\nu(P,T)}\right)^{2n-1}, \quad (3)$$

with $\rho_0 = 1.2041\,\text{kg/m}^3$, $\nu_0 = 1.5083 \cdot 10^{-5}\text{m}^2/\text{s}$, $\rho(P,T) = P/(287.055\,T)$, $\mu(T) = 3.7143\,10^{-6} + 4.9286 \cdot 10^{-8}\,T$ and $\nu(P,T) = \mu(T)/\rho(P,T)$. Fig. 1 shows $K_a(P,T)$ for the limiting cases $n = 0.5$ and $n = 1$ with $P = 101325\,\text{Pa}$. Since $K_a$ is close to one for the expected temperature range, we will use $K_a = 1$ for all temperatures. Furthermore, the air density in (2) should be evaluated at the temperature and pressure of the medium that flows through the orifice. However, if the air temperature is different on either side of the orifice, then the derivative $d\dot{V}/d\Delta P$ of (1b) is discontinuous at $\Delta P = 0$. We prevent this discontinuity by setting $\widetilde{\rho} = 1.2\,\text{kg/m}^3$ in the orifice equation (2), independent of the temperature and pressure. Thus, we implemented (2) in Modelica using the powerlaw (1) with

$$k = C_d A \sqrt{2/\widetilde{\rho}}. \quad (4)$$

## 2.2 Effective Air Leakage Area

ASHRAE Fundamentals [1, p. 25.18] and Clarke [3] list effective air leakage areas for various building construction elements, such as doors, windows and vents. The effective air leakage area tabulated in [1] are based on a reference pressure difference $\Delta P_r = 4\,\text{Pa}$ and a discharge coefficient $C_{d,r} = 1$, but other data sets use $\Delta P_r = 10\,\text{Pa}$ and $C_{d,r} = 0.6$ [4].

We convert the effective air leakage area to the orifice equation (2) as follows. Let $L$ denote the effective air leakage area with units $\text{m}^2$. The area $A$ in the orifice equation (2) is obtained by equating (2) with

$$\dot{V} = C_{d,r}\,L\,\sqrt{2\,\Delta P_r/\rho}, \quad (5)$$

from which follows that

$$A = \frac{C_d}{C_{d,r}}\,L\,\Delta P_r^{0.5-m}. \quad (6)$$

If no value of $m$ is reported with the test results, then Dols and Walton [4] recommend $m = 0.6$ to $m = 0.7$.

## 2.3 Large Vertical Open Aperture

We will now present a model for bi-directional airflow at steady state conditions through a large aperture. The model can be used to compute the bi-directional airflow through open doors or windows. We assume in this section that the aperture is always open. In Sec. 2.4, we extend the model in such a way that the aperture can also be closed.

### 2.3.1 Governing Equations

To deduce the model, we consider an aperture with height $h$ and width $w$ that separates two air volumes (see also Fig. 2). Let $z$ denote the height coordinate, defined so that $z = 0$ at the bottom of the aperture. Let $\bar{P}_A$ and $\bar{P}_B$ denote the static pressures, let $\bar{T}_A$ and $\bar{T}_B$ denote the temperature and let $\bar{\rho}_A$ and $\bar{\rho}_B$ denote the air density in the two air volumes at height $z_A$ and $z_B$. Let $T'_A \triangleq dT_A(z)/dz$ and $T'_B \triangleq dT_B(z)/dz$ denote the vertical temperature gradient in each volume which is assumed to be independent of $z$. We approximate the local air density in volume A at a height $z$ above the bottom of the aperture as

$$\rho_A(z) = \bar{\rho}_A\left(1 - \frac{(z - z_A)\,T'_A}{\bar{T}_A}\right). \quad (7)$$

The static pressure at height $z$ in volume A is

$$P_A(z) = \bar{P}_A + g\int_0^{z_A} \rho_A(s)\,ds - g\int_0^z \rho_A(s)\,ds, \quad (8)$$

where $g = 9.81\,\text{m/s}^2$ is the earth acceleration. Substituting (7) in (8) and evaluating the integrals yields

$$P_A(z) = \bar{P}_A + g\bar{\rho}_A\,(z_A - z) + g\bar{\rho}_A\,\frac{T'_A}{2\,\bar{T}_A}\,\left(z^2 - 2zz_A + z_A^2\right). \quad (9)$$
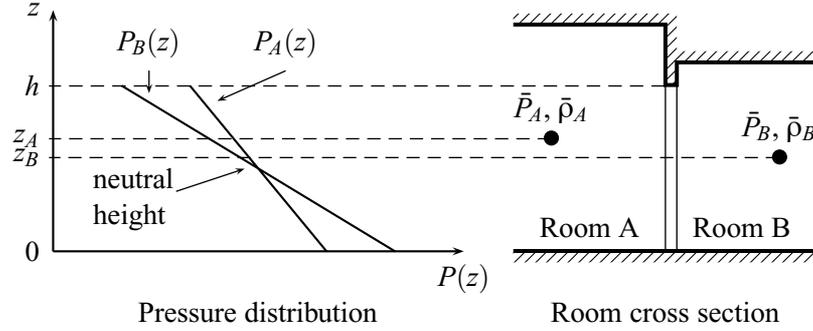
Figure 2: Schematics of two rooms with different heights that are connected by a large vertical opening of height $h$. The left-hand graphics shows schematically the static pressures $P_A(\cdot)$ and $P_B(\cdot)$ as a function of the height $z$ for the situation where $\bar{P}_A < \bar{P}_B$, $\bar{\rho}_A < \bar{\rho}_B$ and without vertical temperature gradient in the rooms. The neutral height is at the point where $P_A(z) = P_B(z)$.

An identical deviation can be done for the static pressure $P_B(z)$. Thus, the static pressure difference at height $z$ is

$$
\begin{aligned}
\Delta P_{AB}(z) &\triangleq P_A(z) - P_B(z) \\
&= \bar{P}_A - \bar{P}_B + g\left(\bar{\rho}_A(z_A - z) - \bar{\rho}_B(z_B - z)\right) \\
&\quad + g\bar{\rho}_A \frac{T_A'}{2\,\bar{T}_A}\left(z^2 - 2zz_A + z_A^2\right) \\
&\quad - g\bar{\rho}_B \frac{T_B'}{2\,\bar{T}_B}\left(z^2 - 2zz_B + z_B^2\right).
\end{aligned} \tag{10}
$$

Equation 10 is a quadratic equation in $z$. Its solutions $z^* \in [0, h]$ that satisfy $\Delta P_{AB}(z^*) = 0$, if they exist, are called the neutral heights. At the neutral heights, there is no flow through the aperture.

The volume flow rate from A to B through the height element $dz$ is for $P_{AB}^m(z) > 0$, $\dot{V}_{AB}(z)/dz = C_d\sqrt{2/\rho_A(z)}\,\Delta P_{AB}^m(z)\,w\,dz$ or else $\dot{V}_{AB}(z)/dz = -C_d\sqrt{2/\rho_B(z)}\,(-\Delta P_{AB}(z))^m\,w\,dz$. The net flow from A to B is

$$
\dot{V}_{AB} = \int_0^h \max(0, d\dot{V}_{AB}(z)/dz)\,dz \tag{11}
$$

and similarly

$$
\dot{V}_{BA} = \int_0^h \min(0, d\dot{V}_{AB}(z)/dz)\,dz. \tag{12}
$$

The exact evaluation of the integrals in (11) and in (12) requires the knowledge of the neutral heights. In the absence of vertical temperature gradients, i.e., if $T_A' = T_B' = 0$, the neutral height is

$$
z^* = \frac{\bar{P}_A - \bar{P}_B + g(\bar{\rho}_A z_A - \bar{\rho}_B z_B)}{g(\bar{\rho}_A - \bar{\rho}_B)}. \tag{13}
$$

CONTAM and IDA neglect vertical temperature gradients and evaluate symbolically the integrals (11)

and (12). Furthermore, in computing the pressure difference across the opening, CONTAM assumes the vertical temperature profile to be constant [4, p. 152], which facilitates in view of the denominator of (13) the numerical solution if $\bar{\rho}_A$ and $\bar{\rho}_B$ are close to each other. In COMIS [6], however, the opening is discretized along the height coordinate to eliminate the need for solving the pressure difference equation (10) for the neutral height. The total flow is then obtained by summation of the flows for the whole opening.

### 2.3.2 Model Discretization

As in COMIS, we also select a discretized model to implement an approximate solution of (11) and (12) since we expect the discretized model to be numerically more robust than an implementation of the analytical solution of (11) and (12) which requires solving (10) for the neutral height which may have zero, one or two solutions in $[0, h]$.

For a fixed $n \in \mathbb{N}$, we discretize the height $h$ of the door into $n$ compartments of equal height $\Delta h = h/n$. For $i \in \{1, \ldots, n\}$, we define $z_n^i \triangleq h(i - 1/2)/n$. We use the orifice equation (2) to compute the flow in each compartment. For sufficiently large positive pressure differences, the orifice equation in each compartment is

$$
\dot{V}_{AB,n}^i = C_d\,w\,\frac{h}{n}\sqrt{\frac{2}{\rho_A(z_n^i)}}\,\Delta P_{AB}^m(z_n^i), \tag{14}
$$

where $\Delta P_{AB}(z_n^i)$ is defined in (10). We implement the orifice equation using the powerlaw relation (1) with

$$
k = C_d\,w\,\frac{h}{n}\sqrt{\frac{2}{\bar{\rho}}}, \tag{15}
$$

where $\hat{\rho} \triangleq (\bar{\rho}_A + \bar{\rho}_B)/2$. In (15), we used the average

of the density at the two reference points A and B to approximate the density in $dz$. As mentioned earlier, the density in $dz$ depends on the flow direction, but using the density of the inflowing medium would cause the volume flow rate to be non-differentiable with respect to the pressure difference at $\Delta P_{AB}^m(z) = 0$. In this model, we know the density on both sides of the aperture and hence use their average value rather than a constant density. In the current implementation, we neglect the vertical temperature gradient in volume A and B and set $T'_A = T'_B = 0$. The model could be extended with little effort to take into account a temperature gradient by adding the quadratic terms in the implementation of the pressure difference equation (10). Extending the model may be important if a room has a displacement ventilation, since vertical temperature gradients can have a major influence on the heat exchange by interzonal airflows [8].

In order to formulate a once continuously differentiable approximation to the $\max(\cdot, \cdot)$ and $\min(\cdot, \cdot)$ functions in (11) and in (12), we compute the average velocity in each compartment as

$$v_n^i \triangleq \frac{\dot{V}_{AB,n}^i}{wh/n}. \tag{16}$$

The net flow from A to B and from B to A through each element is computed as

$$\vec{V}_{AB,n}^i = \dot{V}_{AB,n}^i \, \widetilde{H}(v_n^i; v_\varepsilon), \tag{17a}$$

$$\vec{V}_{BA,n}^i = -\dot{V}_{AB,n}^i + \vec{V}_{AB,n}^i, \tag{17b}$$

where $\widetilde{H}(\cdot; v_\varepsilon)$ is a once continuously differentiable approximation to the Heaviside function, implemented using the Dymola built-in function `spliceFunction`, parametrized by a user specified smoothing parameter $v_\varepsilon$. Good numerical performance has been obtained with $v_\varepsilon = 0.001\,\mathrm{m/s}$.

## 2.4 Large Vertical Operable Aperture

We will now combine the model for the effective air leakage area, presented in Sec. 2.2, and the model for large vertical open apertures, presented in Sec. 2.3, to construct a model for a large aperture that can be open or closed, depending on an input signal. As in the model for the open aperture, we discretize the opening in $n$ horizontal segments, and compute the pressure difference $\Delta P_{AB}(z)$ in each compartment using (10). Let $y \in [0, 1]$ be an input signal, defined such that the aperture is closed if $y = 0$ and open if $y = 1$. We combine the two models by using a linear combination of the flow constants $k$ and the flow exponents

$m$ of each model. In particular, in view of (6) and (4), we set for the closed aperture

$$k_{clo} = \frac{1}{n} C_d \frac{C_d}{C_{d,r}} L \, \Delta P_r^{0.5-m} \sqrt{\frac{2}{\widehat{\bar{\rho}}}} \tag{18}$$

where $n$ is the number of compartments and $\widehat{\rho} \triangleq (\bar{\rho}_A + \bar{\rho}_B)/2$, and we set for the open aperture

$$k_{ope} = \frac{1}{n} C_d \, wh \sqrt{\frac{2}{\widehat{\bar{\rho}}}}. \tag{19}$$

In both models, the flow exponent $m$ is a user-specified parameter which we denote by $m_{clo}$ and $m_{ope}$. The effective flow constant and flow exponent is computed as

$$k = y k_{ope} + (1-y) k_{clo}, \tag{20}$$

$$m = y m_{ope} + (1-y) m_{clo}. \tag{21}$$

We do not claim that this model is able to describe accurately the flow through a half opened door by setting $y = 1/2$. However, for numerical reasons, to change the aperture from open to closed, it may be better to vary the input signal $y$ continuously in time as opposed to using a step function.

## 2.5 Pressure of a Medium Column

This model can be used to model the static pressure of a medium column. The model computes the difference between the static pressure at the bottom $P_b$ and the top $P_t$ of a vertical medium column of height $h$ as

$$P_b = P_t + h \rho g, \tag{22}$$

where the density $\rho$ is a user input and $g = 9.81\,\mathrm{m/s}^2$ is the earth acceleration.

# 3 Implementation in Modelica

We implemented the models using Modelica 2.2 [16] and Modelica_Fluid [5]. All models use one or several instances of a model that implements the power law (1) to define the relationship between flow and pressure difference. Fig. 3 and Fig. 4 show the class hierarchy of the models with one- and two-directional flow, and how the different models relate to the physical description described in the previous sections.
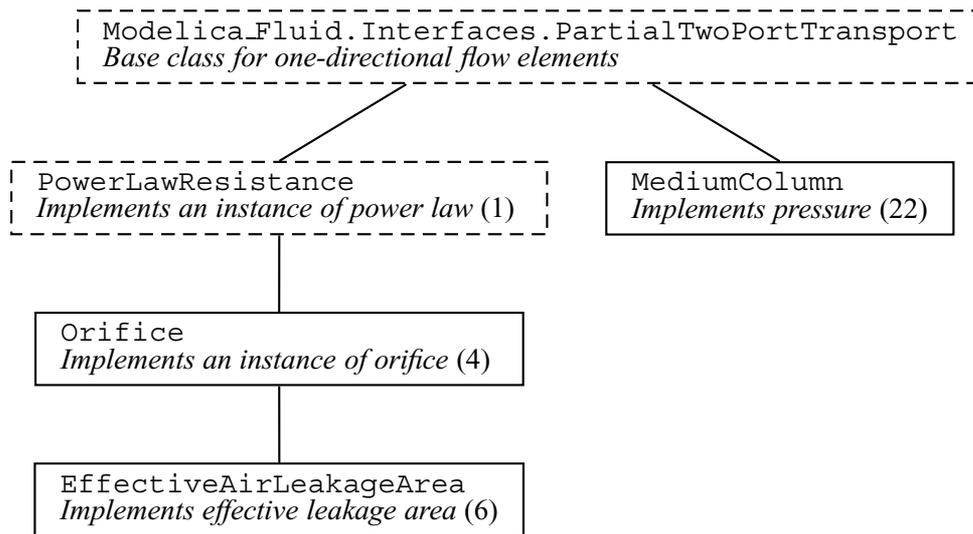
Figure 3: Class hierarchy of models with one-directional flow. The dashed models are partial models.
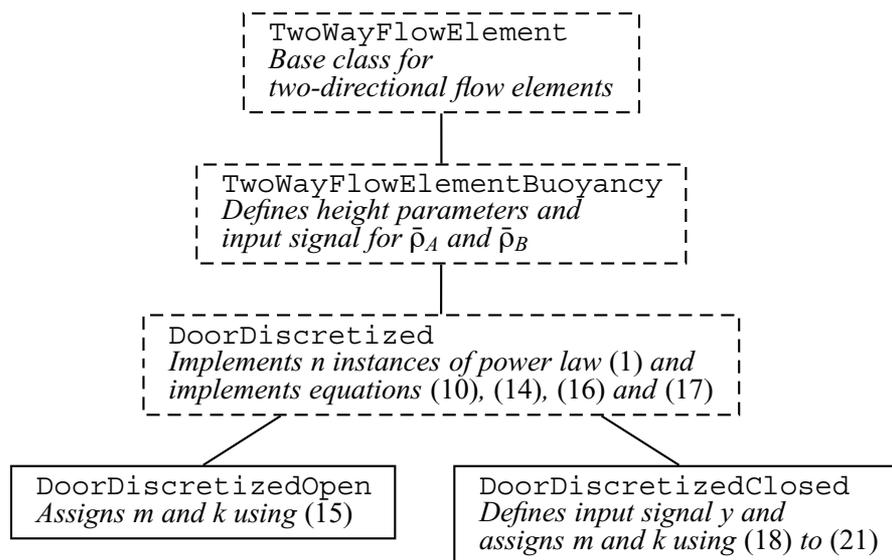


Figure 4: Class hierarchy of models with two-directional flow. The dashed models are partial models.

Table 1: Parameters of the flow elements.

|  | Orifice | Door |
|---|---|---|
| Discharge coefficient $C_D$ | 0.65 | 0.78 |
| Flow coefficient $m$ | 0.5 | 0.78 |
| Transition to linear pressure law $\Delta P_{0,\varepsilon}$ in Pa | 0.1 | 0.1 |
| Area $A$ in $m^2$ | 0.01 | 2.2 |
| Width $w$ in m | - | 1 |
| Height $h$ in m | - | 2.2 |
| Number of compartments $n_{com}$ | - | 10 |
| Minimum velocity $v_\varepsilon$ in m/s | - | 0.001 |

Table 2: Mass flow rates in kg/s computed by CON-TAM and by Modelica.

| Flow element | CONTAM | Modelica |
|---|---|---|
| door West to East | 0.4103 | 0.4184 |
| door East to West | 0.4146 | 0.4228 |
| opening WT | 0.0044 | 0.0044 |
| opening ET | 0.0044 | 0.0044 |
| opening OB | 0.0080 | 0.0080 |
| opening OT | 0.0080 | 0.0079 |

## 4 Comparative Model Validation

We will now compare the buoyancy driven air flow rates through orifices and open doors that were computed in Modelica using Dymola 5.3b with the ones computed in CONTAMW 2.1. The computations were done on a Windows 2000 computer.

Fig. 5 shows a side view of the three rooms used in the validation, Fig. 6 shows the implementation in Dymola and Tab. 1 shows the parameters used to describe the flow paths. In the Modelica computations, the parameter $\Delta P_{0,\varepsilon}$ used in the smoothing described in (1) was set to 0.1 Pa and we used $\widetilde{\rho} = 1.2\,kg/m^3$ in the orifice equation (2).

Tab. 2 lists the mass flow rates computed by CON-TAMW and by Modelica. The door model has the biggest difference in mass flow rate. However, the difference is only 2%, and hence the CONTAM and Modelica model agree within the accuracy expected by the model simplification, such as the assumption of constant density in the flow path and the discretization of the door height.

## 5 Conclusions

Using an object-oriented equation-based modeling language allowed a rapid implementation of a library with multizone air flow models that can be connected to thermal building models. A comparative model validation of the buoyancy driven steady-state mass flow rates in a two storey building between our models and CONTAM showed agreement of the mass flow rates within 2%. This deviation is significantly smaller than the uncertainty associated with selecting model parameters. Large uncertainty in model parameters exist in the selection of the discharge coefficient, the flow exponent and the equivalent leakage area of cracks in the building envelope.

From a computational point of view, smoothing the equations to convert them into once continuously differentiable equations was critical. Without smoothing, the solver failed in some examples to solve the system of equations.

## 6 Acknowledgments

## 7 Nomenclature

### 7.1 Conventions

1. Vectors elements are denoted by superscripts.

2. $f(\cdot)$ denotes a function where $(\cdot)$ stands for the undesignated variables. $f(x)$ denotes the value of $f(\cdot)$ for the argument $x$.

### 7.2 Symbols

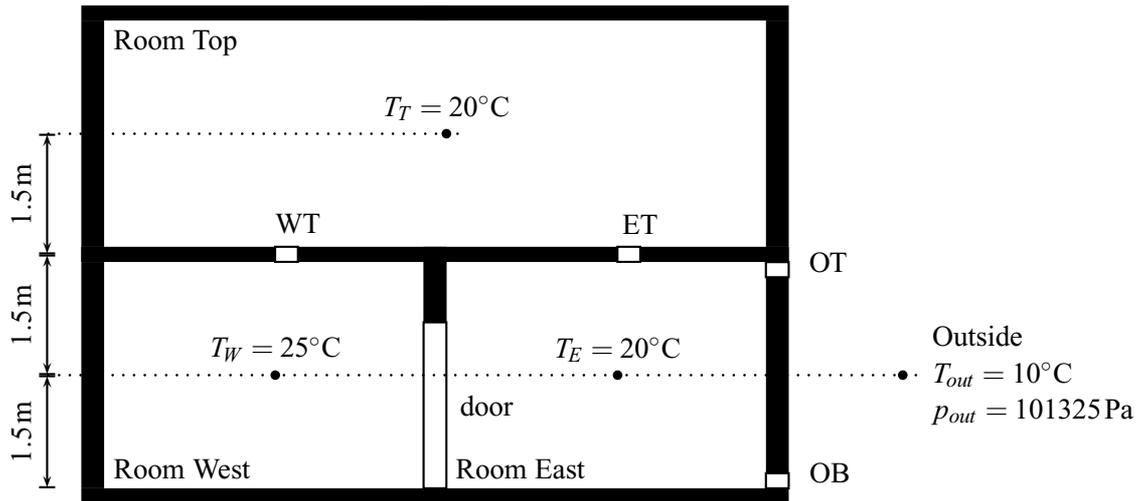| | |
|---|---|
| $a \in A$ | $a$ is an element of $A$ |
| $\mathbb{N}$ | $\{1,2,3,\dots\}$ |
| $\triangleq$ | equal by definition |

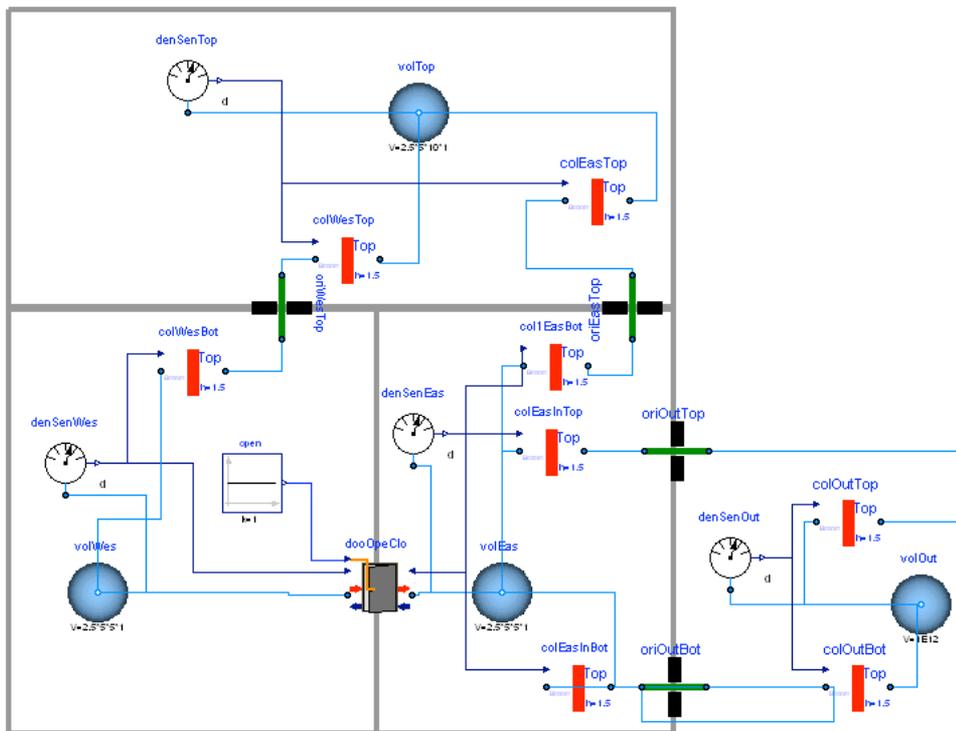Figure 5: Side view of the three rooms used in the validation study.



Figure 6: Implementation of the three room problem that was used for the comparative program validation. The green flow paths are orifice models that implement the model of Section 2.1, the red bars are medium column models that implement the model of Section 2.5, and the gray rectangle is the door model of Section 2.3 and 2.4.

# References

[1] ASHRAE. *Fundamentals*. American Society of Heating, Refrigeration and Air-Conditioning Engineers, 1997.

[2] Axel Bring and Per Sahlin. Modelling air flows and buildings with NMF and IDA. In *Proc. of the 3-rd IBPSA Conference*, pages 463–469, Adelaide, Australia, August 1993.

[3] Joe A. Clarke. *Energy Simulation in Building Design*. Butterworth-Heinemann, Oxford, UK, 2nd edition, 2001.

[4] W. Stuart Dols and George N. Walton. CONTAM 2.0 user manual, multizone airflow and contaminant transport analysis software. Technical Report NISTIR 6921, National Institute of Standards and Technology, November 2002.

[5] Hilding Elmqvist, Hubertus Tummescheit, and Martin Otter. Object-oriented modeling of thermo-fluid systems. In Peter Fritzson, editor, *Proceedings of the 3rd Modelica conference*, pages 269–286, Linköping, Sweden, November 2003. Modelica Association and Institutionen för datavetenskap, Linköpings universitet.

[6] Helmut E. Feustel. COMIS - an international multizone air-flow and contaminant transport model. Technical Report LBNL-42182, Lawrence Berkeley National Laboratory, Berkeley, CA, USA, August 1998.

[7] Helmut E. Feustel and Juergen Dieris. A survey of airflow models for multizone structures. *Energy and Buildings*, 18:79–100, 1992.

[8] J. L. M. Hensen, J. van der Maas, and A. Roos. Air and heat flow through large vertical openings. In *Proc. of the 3-rd IBPSA Conference*, pages 479–485, Adelaide, Australia, August 1993.

[9] Joe Huang, Frederick C. Winkelmann, Frederick F. Buhl, Curtis O. Pedersen, Daniel E. Fisher, Richard J. Liesen, Russell D. Taylor, Richard K. Strand, Drury B. Crawley, and Linda K. Lawrie. Linking the COMIS multi-zone airflow model with the EnergyPlus building energy simulation program. In *Proc. of the 6-th IBPSA Conference*, volume II, pages 1065–1070, Kyoto, Japan, September 1999.

[10] Christian Inard, Hassan Bouia, and Pascal Dalicieux. Prediction of air temperature distribution in buildings with a zonal model. *Energy and Buildings*, 24(2):125–132, July 1996.

[11] D. E. Kiel and D. J. Wilson. Gravity driven flows through open doors. In *7th AIVC Conference*, Stratford on Avon, UK, September 1986. Air Infiltration and Ventilation Centre.

[12] David M. Lorenzetti. Assessing multizone airflow software. Technical Report LBNL-47653, Lawrence Berkeley National Laboratory, Berkeley, CA, USA, December 2001.

[13] B. M. Mahajan. Measurement of interzonal heat and mass transfer by natural convection. *Solar Energy*, 38:437–446, 1987.

[14] B. M. Mahajan and D. D. Hill. Interzonal natural convection for various aperture configurations. In *ASME Winter Annual Meeting*, Anaheim, CA, 1986. American Society of Mechanical Engineers.

[15] Timothy P. McDowell, Steven Emmerich, Jeff W. Thornton, and George N. Walton. Integration of airflow and energy simulation using CONTAM and TRNSYS. *ASHRAE Transaction*, 109(1):1–14, 2003.

[16] Modelica Association. *Modelica – A Unified Object-Oriented Language for Physical Systems Modeling, Language Specification, Version 2.2*, February 2005.

[17] S. B. Riffat. A study of heat and mass transfer through a doorway in a conventional house. Technical Report AIVC 2454, Research in Building Group, Polytechnic Central London, January 1988.

[18] Per Sahlin. On the effects of decoupling airflow and heat balance in building simulation models. *ASHRAE Transaction*, 109(2):788–800, 2003.

[19] Per Sahlin and Axel Bring. IDA solver – A tool for building and energy systems simulation. In J. A. Clarke, J. W. Mitchell, and R. C. Van de Perre, editors, *Proc. of the IBPSA Conference*, Nice, France, August 1991.

[20] J. van der Mass, C. A. Roulet, and J. A. Hertig. Some aspects of gravity driven air flow through large apertures in buildings. *ASHRAE Transactions*, 95(2):573–583, 1989.

[21] George N. Walton. Airflow network models for element based building airflow modeling. *ASHRAE Transactions*, 95(2):611–620, 1989.

[22] Andreas Weber, Markus Koschenz, Viktor Dorer, Marion Hiller, and Stefan Holst. TRNFLOW, a new tool for the modeling of heat, air and pollutant transport in buildings within TRNSYS. In R. Lamberts, C. O. R. Negrão, and J. Hensen, editors, *Proc. of the 7-th IBPSA Conference*, volume III, pages 1363–1368, Rio de Janeiro, Brazil, August 2001.

[23] Michael Wetter. Multizone building model for thermal building simulation in modelica. In *Submitted to: Modelica conference 2006*, Vienna, Austria, September 2006. Modelica Association.